Solvation Dynamics Probed by Femtosecond Transient Absorption Spectroscopy: Vibrational Cooling and Conformational Relaxation in S_1 trans-4,4′-Diphenylstibene†

Xin Tan‡ and Terry L. Gustafson*

Department of Chemistry, The Ohio State University, 100 West 18th Avenue, Columbus, Ohio 43210-1185

Christophe Lefumeux, Gotard Burdzinski, Guy Buntinx,* and Olivier Poizat

Laboratoire de Spectrochimie Infrarouge et Raman (LASIR), Centre d'Etudes et de Recherches Lasers et Applications, Université des Sciences et Technologies de Lille, 59655 Villeneuve d'Ascq Cedex, France

Received: August 16, 2001

We present the femtosecond transient absorption spectra of *trans*-4,4′-diphenylstibene (DPS) in dioxane, methylene chloride, and acetonitrile. The transient absorption spectra feature two bands that are assigned to different electronic transitions. We interpret the spectral changes in the transient absorption spectra in terms of vibrational cooling and conformational dynamics. Vibrational cooling is evidenced by changes in the integrated peak intensity of the transient absorption spectra. For the two transient absorption bands observed in S_1 DPS, the vibrational cooling time constants correlate well with the thermal diffusivity of the solvent. The vibrational cooling rates for the two absorption bands are statistically different in all solvents. We attribute this difference to the relative energy exchange rates between the weighted average of the vibrational modes in the Franck−Condon region that contribute to the S_1-S_n transition and the weighted average of the vibrational modes that contribute to the S_1-S_m transition. On the basis of the present transient absorption data and previous transient Raman data, we suggest that the Franck−Condon region for the S_1-S_n transition has a significant contribution from the phenyl−phenyl portion of DPS; the S_1-S_m transition is likely more localized on the stilbene portion of DPS. The results from the conformational dynamics are consistent with this interpretation. Conformational dynamics are evidenced by peak position shifts in the transient absorption spectra. Only the S_1-S_n transition undergoes significant peak shifts with delay. We attribute the conformational change to the transition from a nonplanar (ground state) to planar (excited state) structure between the two adjacent phenyl rings in DPS.

Introduction

Superimposed upon the fundamental photophysics of molecules in solution are the effects of the microscopic solvent environment. Time-resolved absorption, fluorescence and vibrational spectroscopy have been used extensively to probe the effect of solvent on excited-state relaxation processes.[1−30] Transient resonance Raman spectroscopy has been shown to provide mode-specific details of solvent-induced structural changes for a variety of probe molecule.[1−4,6−8,10−13,26] Transient absorption and transient Raman spectra can provide complementary information on vibrational and conformational dynamics of a probe molecule in differing solvent environments.[4,6,7,12,28−30] In general, multiple time-resolved spectroscopic methods are necessary to gain a more complete understanding of the various relaxation processes, including vibrational cooling, conformational relaxation and solvent reorganization because they all occur on similar time scales.

We have previously used the picosecond transient Raman spectra of *trans*-4,4′-diphenylstilbene (DPS) to probe the effect of solvent and excess vibrational energy on conformational relaxation and vibrational cooling.[1,3,4] Solvent-dependent, mode-specific dynamical behavior was observed for several Raman bands. Of particular interest were changes in relative intensity with delay for certain bands, depending upon both pump and probe wavelength. We interpreted these data as an evolving S_1 state with conformational relaxation and vibrational cooling occurring on the S_1 potential surface.[1,4] If our interpretation is correct, then we should also observe dynamical changes in the transient absorption spectra of DPS. The present femtosecond transient absorption study is intended to confirm the above hypothesis and to obtain additional information on solvation dynamics.

In this report, we present a femtosecond transient absorption study of photoexcited DPS in several solvents. The transient absorption spectra feature two distinct bands with differing dynamics. We compare results for S_1 DPS in dioxane, methylene chloride and acetonitrile. We present the peak position and integrated peak area changes as a function of delay in order to examine conformational relaxation and vibrational cooling in each solvent. The peak position change is prominent in the lower-wavelength band, yet insignificant in the higher-wavelength band. The equilibrium peak position of the higher-wavelength band is blue-shifted in polar solvents, implying involvement of dielectric stabilization. The integrated peak area as a function of delay yields vibrational cooling time constants

† Part of the special issue "Mitsuo Tasumi Festschrift".

* To whom correspondence should be addressed. E-mail: gustafson@chemistry.ohio-state.edu, Guy.Buntinx@univ-lille1.fr.

‡ Present Address: Battelle/PNNL for the USDOE, P. O. Box 999, MSIN: K8-88, Richland, WA 99352.

10.1021/jp013176b CCC: $22.00
Published on Web 03/08/2002

and the lifetime of S_1 DPS in the various solvents. Conformational dynamics and vibrational cooling are essentially complete within 60 ps after photoexcitation, and are slightly more rapid in dioxane and acetonitrile than in methylene chloride. The observed conformational dynamics and vibrational cooling are compared to previous time-resolved resonance Raman and fluorescence data.

Experimental Section

The apparatus for obtaining the femtosecond transient absorption measurements has been previously described.[28,30] Briefly, a Ti−sapphire based femtosecond laser system, consisting of a Ti:sapphire oscillator (MIRA 900D, Coherent) pumped by a 12-W cw argon laser (INNOVA 310, Coherent) and a regenerative amplifier (ALPHA 1000, BM Industries) pumped by a 10-W 1-kHz intracavity frequency-doubled Nd:YLF laser (621D, BM Industries), provides 1-mJ, 90-fs pulses at ∼800 nm. The majority of the energy from the fundamental was frequency tripled to provide 266-nm pump excitation. A small portion (a few microjoules) of the fundamental energy was used to generate a white light continuum probe in a CaF_2 plate. The continuum probe pulse was delayed in time relative to the pump pulse using an optical delay line. The probe polarization was set at the magic angle (54.7°) with respect to the polarization of the pump beam. The white light continuum probe was split into two parallel beams and directed to the sample cell. One of the two beams was overlapped in the sample with the 266-nm excitation beam and the other was used as the reference beam. Both continuum beams were imaged into a single spectrograph equipped with a CCD detector (Princeton Instruments). The optical density of the photoexcited sample at various delay times was obtained using the ratio of the intensity of the white light spectrum from the photoexcited region (I) and the intensity of the white light spectrum from the unexcited region (I_0). The spectra were recorded over the range from ∼390 to ∼780 nm.

DPS was purchased from Lancaster Chemical (Scintillation grade, 2039−68−1) and was used without further purification. Solvents of spectrophotometric grade were obtained from S. D. S. (France). Solutions of DPS in dioxane and methylene chloride were prepared with a concentration of 0.54 mM and 0.48 mM, respectively. A saturated solution of DPS in acetonitrile with a concentration less than 0.5 mM was used.

Results

Femtosecond transient absorption spectra were collected for DPS in several solvents with a pump wavelength of 266 nm and the white-light continuum probe. In Figure 1, we present the steady-state absorption and emission spectra, and the transient absorption spectra of DPS in acetonitrile at a series of representative delays following photoexcitation. The transient absorption spectra feature two positive absorption bands (at ∼630 and ∼730 nm), and a negative stimulated emission band that mirrors the fluorescence (at ∼400 nm). The transient absorption bands show changes in peak position, spectral intensity and bandwidth with respect to time delay. In Figure 2, we expand the region containing the two transient absorption bands for a series of normalized spectra of DPS in (a) dioxane, (b) methylene chloride and (c) acetonitrile. Both spectral shift and bandwidth variations are evident for the lower-wavelength band (at ∼630 nm). The early time spectra are red-shifted and broadened compared to spectra at longer delays. For the higher-wavelength band (at ∼730 nm), however, the dominant effect is delay-dependent band narrowing.

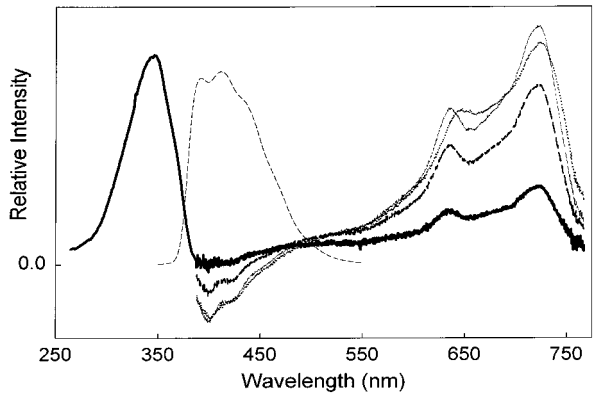

Figure 1. Steady-state absorption and emission, and femtosecond transient absorption spectra of *trans*-4,4′-diphenylstilbene (DPS) in acetonitrile. The smooth and thick solid curve is the steady-state absorption spectrum and the short-dashed curve next to it is the fluorescence emission spectrum. The flat dotted hairline is the transient absorption spectrum taken at negative delay of −1 ps. The dotted, thin-solid, long-dashed and thick-solid curves represent the transient absorption spectra taken at delays of 5, 50, 500, and 1000 ps, respectively.

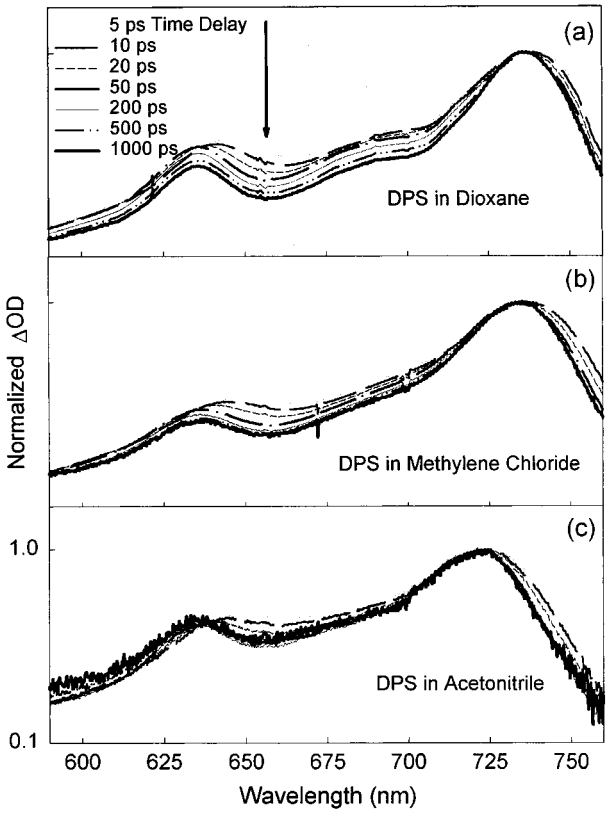

Figure 2. Delay-dependent spectral shift and bandwidth variation of the transient absorption spectra normalized to the higher-wavelength band. The dotted, long-dashed, short-dashed, dash−dotted, solid-hairlined, dash−dot-dotted, and thick-solid-lined curves represent the transient absorption spectra measured at time delays of 5, 10, 20, 50, 200, 500, and 1000 ps, respectively, for DPS in (a) dioxane, (b) methylene chloride, and (c) acetonitrile.

We quantified the changes in the peak position and the changes in the integrated peak area with delay by fitting the normalized transient absorption spectra using Gaussian line shapes. We note that we used the integrated peak area and not the bandwidth to quantify one aspect of the dynamics. There was no statistical difference between the two measurements, but the integrated peak area gave smaller uncertainties. We also

TABLE 1: Equilibrium Peak Position of the Two Transient Absorption Bands in Comparison to the Dielectric Constant of the Solvent

solvent	dielectric constant[a]	S_1-S_n transition equilibrium peak position (nm)	S_1-S_m transition equilibrium peak position (nm)
Dioxane	2.209	632.3 ± 0.1	739.2 ± 0.2
Methylene Chloride	9.08	630.1 ± 0.1	739.0 ± 0.4
Acetonitrile	36.7	629.8 ± 0.6	726.2 ± 1.1

[a] Ref 53

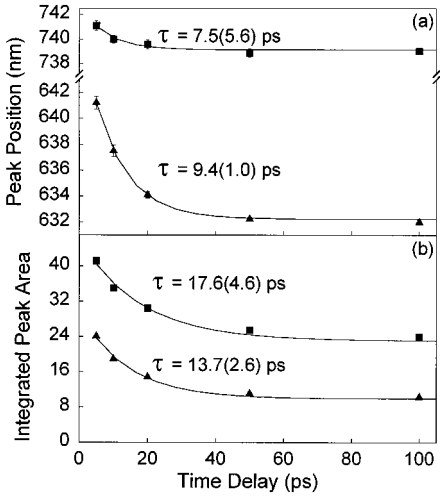

Figure 3. Peak position and peak area changes of normalized transient absorption bands for DPS in dioxane. (▲) and (■) represent the lower-wavelength (S_1-S_n) and higher-wavelength (S_1-S_m) transient bands, respectively. (a) Peak position as a function of delay. (b) Integrated peak area as a function of delay. The solid lines are best fits to the data.

note that Gaussian line shapes fit the data well at all delay times. In Figures 3, 4, and 5, we present the delay-dependent changes of the two transient absorption bands for DPS in dioxane, methylene chloride and acetonitrile, respectively, over the first 100 ps delay. The error bars represent ± 2*s* in the fits. The dynamical peak shift and band shape changes are essentially complete within 60 ps following photoexcitation.

In Figures 3a, 4a, and 5a, we observe that the dynamics of the peak position change are fundamentally different for the two transient absorption bands. The lower-wavelength band displays a prominent shift (>10 nm) over the first 50 picoseconds in all solvents. For the higher-wavelength band, however, the peak position shifts only slightly (<2 nm) with delay in dioxane, but remains almost constant in methylene chloride and acetonitrile. The peak position changes for the lower-wavelength band can best be fit by a single-exponential decay function with an offset, corresponding to the equilibrium position. The relaxation time constants were calculated to be 9.4 ± 1.0, 12.7 ± 0.9, and 9.5 ± 2.9 ps for DPS in dioxane, methylene chloride, and acetonitrile, respectively. The equilibrium peak position for the lower-wavelength band is only slightly dependent upon solvent (632.3 ± 0.1 nm in dioxane; 630.1 ± 0.1 nm in methylene chloride; 629.8 ± 0.6 nm in acetonitrile). For the higher-wavelength band, however, the equilibrium peak position undergoes a blue shift between nonpolar solvents (739.2 ± 0.2 nm in dioxane; 739.0 ± 0.4 nm in methylene chloride) and polar solvent (726.2 ± 1.1 nm in acetonitrile). In Table 1, we compare the equilibrium peak positions of the transient absorption bands with the dielectric constant of each solvent.

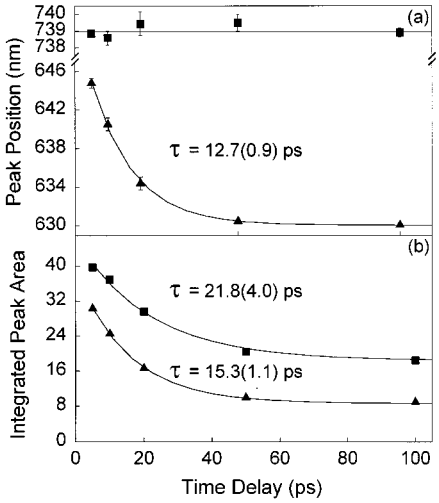

Figure 4. Peak position and peak area changes of normalized transient absorption bands for DPS in methylene chloride. (▲) and (■) represent the lower-wavelength (S_1-S_n) and higher-wavelength (S_1-S_m) transient bands, respectively. (a) Peak position as a function of delay. (b) Integrated peak area as a function of delay. The solid lines are best fits to the data.

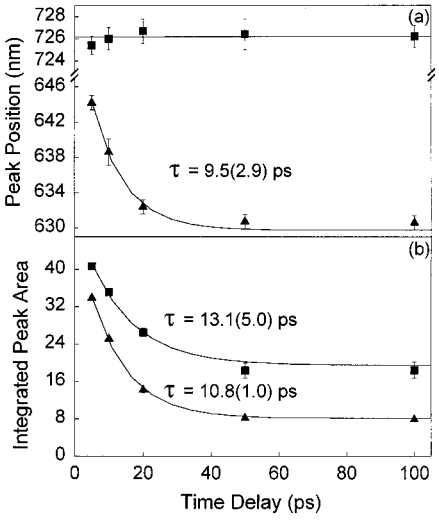

Figure 5. Peak position and peak area changes of normalized transient absorption bands for DPS in acetonitrile. (▲) and (■) represent the lower-wavelength (S_1-S_n) and higher-wavelength (S_1-S_m) transient bands, respectively. (a) Peak position as a function of delay. (b) Integrated peak area as a function of delay. The solid lines are best fits to the data.

In Figure 6, we present the integrated peak areas for both transient absorption bands in (a) dioxane, (b) methylene chloride and (c) acetonitrile over the delay range from 0 to 1500 ps. The integrated peak area changes follow biexponential dynamics. The long component represents the decay of the excited-state population. The solid line in each curve is the best fit to a biexponential decay. The longer-lived component is ∼1 ns, consistent with the S_1 lifetime of DPS.[5] To focus on the short time component, the data presented in Figures 3b, 4b, and 5b have used the integrated peak areas from the normalized transient absorption bands. This procedure eliminates the long-lived (population) decay from the fast dynamics. The time constants for the fits of the normalized integrated peak areas for both absorption bands in each solvent and the thermal diffusivity of the solvents are presented in Table 2. The decay time constants are statistically different (at the 95% confidence

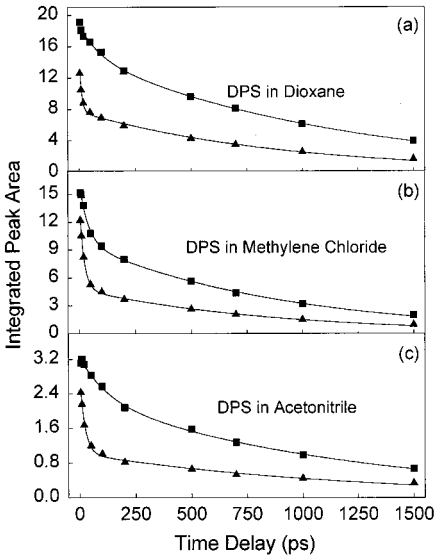

Figure 6. Integrated peak areas as function of time delays obtained from the original unnormalized transient absorption spectra of DPS in (a) dioxane, (b) methylene chloride, and (c) acetonitrile. (▲) and (■) represent the lower-wavelength (S_1-S_n) and higher-wavelength (S_1-S_m) transient bands, respectively. The solid lines are best fits to the data.

TABLE 2: Vibrational Cooling Times of DPS in Various Solvents in Comparison with Solvent Thermal Diffusivity

solvent	thermal diffusivity[a] κ (x 10^{-8} m^2/s)	vibrational cooling time constant[b](ps)	vibrational cooling time constant[c](ps)
Methylene Chloride	8.806	15.3 ± 1.1	21.8 ± 4.0
Dioxane	8.91	13.7 ± 2.6	17.6 ± 4.6
Acetonitrile	10.7	10.8 ± 1.0	13.1 ± 5.0

[a] $\kappa = \lambda \cdot M/C_p \cdot r$ [b] The lower-wavelength (higher-energy) transient absorption band (S_1-S_n). [c] The higher-wavelength (lower-energy) transient absorption band (S_1-S_m).

level) between the two transient absorption bands in each solvent.

Discussion

DPS is an interesting molecule for probing solvent effects on excited-state dynamics for several reasons. It has a long-lived S_1 state, making it possible to obtain high quality absorption and Raman spectra to long delays; the transient absorption cross section is large, based on the intensity of the excited-state Raman spectra; and there appear to be conformational changes (i.e., nuclear coordinate changes in the excited state) that occur on time scales comparable to vibrational cooling.[1,3,4] Our current understanding of the excited state dynamics has been based primarily on picosecond transient Raman data.[1,3,4] The current picture for the photophysical processes of DPS in the S_1 electronic state is as follows.[4] After the initial photoexcitation, the excess vibrational energy initially stored in the Franck−Condon modes of the molecule is redistributed in less than ~100 fs and deposited in the first solvent shell.[4,6,31−33] Following this ultrafast vibrational cooling, slower processes (~10−50 ps) ensue, including vibrational cooling in which the"hot" first solvent shell cools by transferring energy to the bulk solvent and conformational relaxation in which the solute changes its conformation along certain nuclear coordinates in order to relax to the optimum equilibrium geometry in the excited state.[1,3,4,6,31−33] Femtosecond transient absorption spectra provide markers (changes in peak position and bandwidth) for the vibrational and conformational relaxation of an evolving S_1 state. We assign the two transient absorption bands (at ~630 and 730 nm) to different electronic transitions. The higher-wavelength (lower-energy) absorption band represents the transition from S_1 to S_m, and the lower-wavelength (higher-energy) absorption band represents the transition from S_1 to S_n, where S_n is a higher energy electronic excited state than S_m. The assignment is consistent with the results of transient Raman experiments probing into the two transient absorption bands that reveal different resonance enhancement patterns characteristic of different electronic transitions.[34]

Vibrational Cooling. The band shapes for both electronic transition bands (S_1-S_n) and (S_1-S_m) evidence peak shifts and band narrowing with delay. Band narrowing in transient absorption spectra has been consistently interpreted as vibrational cooling.[12,28,30,35,36] We have chosen to use the integrated peak area of the normalized transient absorption bands to quantify the vibrational cooling dynamics. This procedure eliminates the long-lived (population) decay. (See Figures 3b, 4b, and 5b for DPS in dioxane, methylene chloride, and acetonitrile, respectively.) The results of the fits of the fast decay component are presented in Table 2.

There are two main features of the vibrational cooling data. First, the vibrational cooling time constants correlate with the thermal diffusivity of the solvent, consistent with the model proposed by Iwata and Hamaguchi to interpret vibrational cooling as observed in picosecond transient Raman spectra.[6,31−33] Vibrational cooling of S_1 DPS is fastest in acetonitrile which has the highest thermal diffusivity (10.7×10^{-8} m^2s^{-1}). The thermal diffusivities of dioxane and methylene chloride are comparable to each other, as are the vibrational cooling rates. The trend in these data is consistent with the trend obtained for vibrational cooling in *trans*-Stilbene (tS) obtained from transient Raman measurements in solvents with similar thermal diffusivities.[31]

It is of interest to compare the vibrational cooling times for DPS obtained from the present transient absorption data to those obtained from picosecond transient Raman measurements.[4] We can compare directly the results for vibrational cooling in S_1 DPS in dioxane and methylene chloride using both measurement techniques. The vibrational cooling times in dioxane and methylene chloride as measured using the olefin C═C stretch band at ~1605 cm^{-1} in S_1 DPS were 6.3 and 36 ps, respectively. These data compare with values of ~15 ps in both solvents as measured with the transient absorption data for the S_1-S_n transition, the band from which the resonance enhancement was derived in the transient Raman spectra. (See Table 2.) We note that there is a difference in the excitation wavelength between the two experiments, 266 nm in the present work and 287 nm in the transient Raman experiment.[4] The transient absorption experiment is placing ~10 600 cm^{-1} of excess vibrational energy above the 0−0 transition for DPS (at ~27 000 cm^{-1}); the transient Raman experiment placed ~7900 cm^{-1} of excess vibrational energy. The results are still surprising because the values from the transient Raman experiment are in different directions relative to the results from the transient absorption measurements for the two solvents. We suggest that this discrepancy between the two measurement methods arises from the fundamental difference in how vibrational cooling is observed by each method. It is well established that the vibrational cooling process as observed in transient Raman spectra occurs via anharmonic coupling of high-frequency vibrational modes to low-frequency modes, which undergo

energy exchange with the solvent.[37,38] Anharmonic coupling accounts for the mode-specific changes observed in the transient Raman spectra of a variety of molecules.[1,4,7,8,11,12,32,33,39−49] Only those high frequency vibrations that couple effectively to the low-frequency vibrations undergo peak position shifts and bandwidth changes with delay, the spectroscopic signature for vibrational cooling in transient Raman spectra. Vibrational cooling as observed in transient absorption spectroscopy samples the ensemble of vibrational modes in the Franck−Condon region of S_1 that couple to the higher electronic excited state. The vibrational cooling times in this case will be the weighted average of all the modes that participate in the transition.

The second major feature of the vibrational cooling data is that the measured vibrational cooling time constants are statistically faster for the higher energy band (S_1-S_n) than the lower energy band (S_1-S_m) in all solvents. This is somewhat unexpected since both transient absorption bands are probing vibrational cooling from the S_1 state. We do know, however, that the Franck−Condon region on the S_1 potential surface of DPS is different for the S_1-S_m and S_1-S_n transitions, based on the present transient absorption spectra and the transient resonance Raman spectra probed in both transitions.[34] Following the same line of reasoning as above, we suggest that the weighted average of the vibrational modes that contribute to the S_1-S_m transition undergo energy exchange at a different rate compared to the rate of energy exchange from the weighted average of the vibrational modes that contribute to the S_1-S_n transition. On the basis of previous transient Raman data,[1,4] the S_1-S_n transition involves a significant displacement in the phenyl−phenyl bond (vide infra). The torsional motions associated with the two phenyl rings becoming coplanar may provide an effective exchange mechanism for vibrational cooling, significantly shortening the time constants as measured in the S_1-S_n transition.

Conformational Relaxation. We have previously interpreted relative intensity changes with delay in the picosecond transient Raman spectra as an indication of conformational dynamics on the evolving S_1 surface of DPS.[1,3,4] The intensities of the Raman bands change because the Franck−Condon overlap with the excited state from which the S_1 bands are deriving their intensity is changing as the nuclear coordinates evolve. If this hypothesis is correct, then we would also expect to observe peak position changes with delay in the femtosecond transient absorption spectra. As evidenced in Figure 2 and clearly shown in Figures 3a, 4a, and 5a, the two transient absorption bands demonstrate different conformational dynamics. The lower-wavelength band (S_1-S_n) shows significant conformational relaxation represented by prominent spectral shift with delay, whereas the higher-wavelength band (S_1-S_m) shows negligible peak shift. These results correlate with picosecond transient resonance Raman spectra, where spectra obtained with excitation into the S_1-S_n band show relative intensity changes with delay for various vibrational modes, whereas spectra obtained with excitation into the S_1-S_m band do not show relative intensity changes.[1,4,34]

The picture that emerges from these data is that the conformational changes we are observing is localized in the phenyl−phenyl portion of DPS. Based on PM3 level quantum chemical calculations,[1] in the ground state the two phenyl rings are ∼30° out of the plane relative to each other. In the excited state, the two phenyl rings are coplanar. Only those S_1 Raman bands that contain a significant contribution from the phenyl−phenyl motion exhibit intensity changes with delay when probed in the region of the S_1-S_n transition.[1,3,4] No intensity changes are observed in the transient Raman bands when probed in the region of the S_1-S_m transition.[34] We can ascribe the peak position changes in the S_1-S_n transient absorption band to the change in the planarity of the two phenyl rings. This interpretation is consistent with the observation of a similar dynamic spectral shift in the femtosecond transient absorption spectra for S_1 quaterphenyl in solution.[12] We note that quaterphenyl also has the potential for undergoing a transition from nonplanar to planar between the ground and excited states.

The time constants for the peak position change in the S_1-S_n band are ∼10 ps in all three solvents as shown in Figures 3a, 4a, and 5a. The conformational relaxation times of the S_1-S_n band are similar in all solvents and do not correlate well with any bulk solvent property. And it is difficult to compare the dynamics of conformational relaxation as probed with transient absorption with the dynamics probed by transient Raman. In the transient Raman spectra the dynamics of conformational relaxation depend on the probe wavelength, owing to the nature of the resonance enhancement process.[4] For example, at a probe wavelength of 630 nm the conformational dynamics are complete within ∼10 ps, using the 1483 cm^{-1} band in S_1 DPS, but at a probe wavelength of 660 nm the conformational dynamics are not complete until a delay of ∼35 ps.[4] We have previously correlated the conformational dynamics as probed by transient Raman intensity changes to the dielectric constant of the solvent.[1,3,4] We suggest that the conformational dynamics as probed in transient absorption spectra are affected by the dielectric constant of the solvent and by the viscosity. Additional experiments in other solvents and across a range of temperatures will be required to evaluate how specific bulk solvent properties influence the dynamics of conformational changes in the excited state.

Although the equilibrium peak position for the lower-wavelength band (S_1-S_n) is unchanged in all the solvents, the equilibrium peak position for the higher-wavelength band (S_1-S_m) undergoes a blue shift (∼13 nm) from nonpolar solvents (dioxane and methylene chloride) to polar solvent (acetonitrile). (See Table 1.) We attribute the equilibrium peak shift of S_1-S_m band in acetonitrile to dielectric stabilization of the S_m state in DPS. The equilibrium peak position of the lower wavelength band (S_1-S_n) is roughly independent of solvent, suggesting that the dielectric stabilization of S_1 and S_n is similar in direction and magnitude. The ground-state absorption spectrum of DPS shows negligible peak shift with solvent,[5] suggesting little dielectric perturbation of the S_1 state. This observation coupled with the transient absorption results implies that both the S_1 and S_n levels are not affected significantly by dielectric stabilization in polar solvents. The blue shift in polar solvent of the higher wavelength band (S_1-S_m) suggests the S_m energy level is raised relative to the S_1 and S_n levels. The S_m state appears to be more perturbed by dielectric stabilization in polar solvents than the S_1 and S_n states.

Conclusions

In this work we have presented the femtosecond transient absorption spectra of DPS in dioxane, methylene chloride and acetonitrile. The transient absorption spectra feature two bands that are assigned to different electronic transitions. We interpret the spectral changes in the transient absorption spectra in terms of vibrational cooling and conformational dynamics. Vibrational cooling is evidenced by changes in the integrated peak intensity of the transient absorption spectra. For the two transient absorption bands observed in S_1 DPS the vibrational cooling time constants correlate well with the thermal diffusivity of the solvent. The vibrational cooling rates for the two absorption

bands are statistically different in all solvents. We suggest that this difference arises because the weighted average of the vibrational modes in the Franck−Condon region that contribute to the S_1-S_n transition undergo energy exchange faster compared to the rate of energy exchange from the weighted average of the vibrational modes that contribute to the S_1-S_m transition. On the basis of the present transient absorption data and previous transient Raman data, we suggest that the Franck−Condon region for the S_1-S_n transition has a significant contribution from the phenyl−phenyl portion of DPS; the S_1-S_m transition is likely more localized on the stilbene portion of DPS. The results from the conformational dynamics are consistent with this interpretation. Conformational dynamics are evidenced by peak position shifts in the transient absorption spectra. Only the S_1-S_n transition undergoes significant peak shifts with delay. We attribute the conformational change to the transition from a nonplanar (ground state) to planar (excited state) structure between the two adjacent phenyl rings in DPS.

One particularly important insight that comes from these data is that the measurement of vibrational cooling time constants in the excited states of molecules depends on the method used. The vibrational time constants measured using transient absorption spectra differ from those obtained from transient Raman measurements in the same solvents. More work remains to clarify the origin of this effect. It would be of interest to measure the dynamic Stokes shift using ultrafast fluorescence spectroscopy to compare to the results from both the transient absorption and transient Raman spectra. Transient anti-Stokes Raman spectra have also been used extensively to monitor vibrational cooling in the excited state.[11,12,43,47,49−52] We have not yet been successful at measuring the transient anti-Stokes Raman spectra of DPS.

Acknowledgment. We acknowledge support for this work from NSF (T.L.G.) and CNRS and CERLA (G.B. and O.P.). The Laboratoire de Spectrochimie Infrarouge et Raman is Unité mixte de Recherche de l'Université de Lille1 et du CNRS (UMR 8516). The Centre d'Etudes et Recherches Lasers et Applications is supported by the Ministère chargé de la Recherche, the Région Nord-Pas de Calais and the Fonds Européen de Développement Economique des Régions.

References and Notes

(1) Butler, R. M.; Lynn, M. A.; Gustafson, T. L. *J. Phys. Chem.* **1993**, *97*, 2609−2617.
(2) Morris, D. L.; Gustafson, T. L. *Appl. Phys. B* **1994**, *59*, 389−395.
(3) Leonard, J. D., Jr.; Gustafson, T. L. *J. Raman Spectrosc.* **2000**, *31*, 353−358.
(4) Leonard, J. D., Jr.; Gustafson, T. L. *J. Phys. Chem. A* **2001**, *105*, 1724−1730.
(5) Tan, X.; Gustafson, T. L. *J. Phys. Chem. A* **2000**, *104*, 4469−4474.
(6) Iwata, K.; Hamaguchi, H. *J. Mol. Liq.* **1995**, *65*−*6*, 417−420.
(7) Iwata, K.; Hamaguchi, H. *Chem. Phys. Lett.* **1992**, *196*, 462−468.
(8) Hester, R. E.; Matousek, P.; Moore, J. N.; Parker, A. W.; Toner, W. T.; Towrie, M. *Chem. Phys. Lett.* **1993**, *208*, 471−478.
(9) Kwok, W. M.; Ma, C.; Phillips, D.; Matousek, P.; Parker, A. W.; Towrie, M. *J. Phys. Chem. A* **2000**, *104*, 4188−4197.
(10) Matousek, P.; Parker, A. W.; Phillips, D.; Scholes, G. D.; Toner, W. T.; Towrie, M. *Chem. Phys. Lett.* **1997**, *278*, 56−62.
(11) Matousek, P.; Parker, A. W.; Toner, W. T.; Towrie, M.; Defaria, D. L. A.; Hester, R. E.; Moore, J. N. *Chem. Phys. Lett.* **1995**, *237*, 373−379.
(12) Matousek, P.; Parker, A. W.; Towrie, M.; Toner, W. T. *J. Chem. Phys.* **1997**, *107*, 9807−9817.
(13) Toner, W. T.; Matousek, P.; Parker, A. W.; Towrie, M. *Lect. Notes Phys.* **1997**, *499*, 151−158.
(14) Blanchard, G. J.; Cihal, C. A. *J. Phys. Chem.* **1988**, *92*, 5950−5954.
(15) Flory, W. C.; Blanchard, G. J. *Appl. Spectrosc.* **1998**, *52*, 82−90.
(16) Goldie, S. N.; Blanchard, G. J. *J. Phys. Chem. A* **1999**, *103*, 999−1006.
(17) Jiang, Y.; Blanchard, G. J. *J. Phys. Chem.* **1994**, *98*, 9411−9416.
(18) Jiang, Y.; Blanchard, G. J. *J. Phys. Chem.* **1995**, *99*, 7904−7912.
(19) Mccarthy, P. K.; Blanchard, G. J. *J. Phys. Chem.* **1996**, *100*, 5182−5187.
(20) Owrutsky, J. C.; Raftery, D.; Hochstrasser, R. M. *Annu. Rev. Phys. Chem.* **1994**, *45*, 519−555.
(21) Castner, E. W., Jr.; Maroncelli, M.; Fleming, G. R. *J. Chem. Phys.* **1987**, *86*, 1090−1097.
(22) Maroncelli, M.; Fleming, G. R. *J. Chem. Phys.* **1987**, *86*, 6221−6239.
(23) Gardecki, J.; Horng, M. L.; Papazyan, A.; Maroncelli, M. *J. Mol. Liq.* **1995**, *65*−*6*, 49−57.
(24) Lewis, J. E.; Maroncelli, M. *Chem. Phys. Lett.* **1998**, *282*, 197−203.
(25) Stratt, R. M.; Maroncelli, M. *J. Phys. Chem.* **1996**, *100*, 12 981−12 996.
(26) Sue, J.; Mukamel, S.; Okamoto, H.; Hamaguchi, H.; Tasumi, M. *Chem. Phys. Lett.* **1987**, *134*, 87−95.
(27) Yamaguchi, S.; Hamaguchi, H. *Chem. Phys. Lett.* **1994**, *227*, 255−260.
(28) Buntinx, G.; Naskrecki, R.; Poizat, O. *J. Phys. Chem.* **1996**, *100*, 19 380−19 388.
(29) Buntinx, G.; Poizat, O.; Leygue, N. *J. Phys.Chem.* **1995**, *99*, 2343−2352.
(30) Buntinx, G.; Naskrecki, R.; Didierjean, C.; Poizat, O. *J. Phys. Chem. A* **1997**, *101*, 8768−8777.
(31) Iwata, K.; Hamaguchi, H. *J. Phys. Chem. A* **1997**, *101*, 632−637.
(32) Iwata, K.; Hamaguchi, H. *J. Raman Spectrosc.* **1998**, *29*, 915−918.
(33) Iwata, K.; Hamaguchi, H. O. *Laser Chem.* **1999**, *19*, 367−370.
(34) Tan, X.; Gustafson, T. L.; Lefumeux, C.; Burdzinski, G.; Buntinx, G.; Poizat, O., unpublished work
(35) Greene, B. I.; Hochstrasser, R. M.; Weisman, R. B. *J. Chem. Phys.* **1979**, *70*, 1247−1259.
(36) Gustafson, T. L.; Kyllo, E. M.; Frost, T. L.; Sun, R. G.; Lim, H.; Wang, D. K.; Epstein, A. J.; Lefumeux, C.; Burdzinski, G.; Buntinx, G.; Poizat, O. *Synth. Met.* **2001**, *116*, 31−34.
(37) Shelby, R. M.; Harris, C. B.; Cornelius, P. A. *J. Chem. Phys.* **1979**, *70*, 34−41.
(38) Marks, S.; Cornelius, P. A.; Harris, C. B. *J. Chem. Phys.* **1980**, *73*, 3069−3081.
(39) Weaver, W. L.; Huston, L. A.; Iwata, K.; Gustafson, T. L. *J. Phys. Chem.* **1992**, *96*, 8956−8961.
(40) Hamaguchi, H.; Gustafson, T. L. *Annu. Rev. Phys. Chem.* **1994**, *45*, 593−622.
(41) Qian, J.; Schultz, S. L.; Bradburn, G. R.; Jean, J. M. *J. Phys. Chem.* **1993**, *97*, 10 638−10 644.
(42) Qian, J.; Schultz, S. L.; Bradburn, G. R.; Jean, J. M. *J. Luminesc.* **1994**, *60*, 1727−1730.
(43) Lingle, R., Jr.; Xu, X.; Zhu, H.; Yu, S. C.; Hopkins, J. B. *J. Phys. Chem.* **1991**, *95*, 9320−9331.
(44) Lingle, R., Jr.; Xu, X.; Zhu, H.; Yu, S. C.; Hopkins, J. B.; Straub, K. D. *J. Am. Chem. Soc.* **1991**, *113*, 3992−3994.
(45) Toner, W. T.; Matousek, P.; Parker, A. W.; Towrie, M. *Laser Chem.* **1999**, *19*, 79−82.
(46) Nakabayashi, T.; Okamoto, H.; Tasumi, M. *J. Raman Spectrosc.* **1995**, *26*, 841−845.
(47) Nakabayashi, T.; Okamoto, H.; Tasumi, M. *J. Phys. Chem. A* **1997**, *101*, 7189−7193.
(48) Nakabayashi, T.; Okamoto, H.; Tasumi, M. *J. Phys. Chem. A* **1997**, *101*, 3494−3500.
(49) Nakabayashi, T.; Okamoto, H.; Tasumi, M. *J. Phys. Chem. A* **1998**, *102*, 9686−9695.
(50) Mizutani, Y.; Kitagawa, T. *Science* **1997**, *278*, 443−446.
(51) Mizutani, Y.; Uesugi, Y.; Kitagawa, T. *J. Chem. Phys.* **1999**, *111*, 8950−8962.
(52) Fujino, T.; Tahara, T. *J. Phys. Chem. A* **2000**, *104*, 4203−4210.
(53) Lide, D. R. *CRC Handbook of Chemistry and Physics*, 74 ed.; CRC Press: Boca Raton, 1993.